LIQUID CRYSTALS, 1998, VOL. 25, NO. 4, 459–465

A comparative laser Raman study on TB4A, TB7A and TB10A

S. K. DASH†, RANJAN K. SINGH‡, P. R. ALAPATI*† and A. L. VERMA‡

†Department of Physics, North Eastern Regional Institute of Science and Technology, Itanagar—791 109, India

‡Department of Physics, North Eastern Hill University, Permanent Campus, Shillong—793022, India

(*Received 22 September 1997; in final form 28 February 1998; accepted 28 February 1998*)

The basic structural differences between three thermotropic liquid crystals TB4A, TB7A and TB10A have been interpreted by analysing their Raman spectra. Three spectral regions, 925–1025, 1275–1475 and 1525–1650 cm^{-1}, have been chosen in this context to incorporate their structural dissimilarity. The induced planarity of the backbone, as an effect of increasing chain length, has been studied by observing the changes in the respective Raman spectra of the three compounds. A tentative assignment of all the modes observed in the region 400–1700 cm^{-1} is made in this context. The molecular conformations of the three compounds have been predicted in their solution states, and are compared with the molecular environment that exists in their liquid crystalline states. Structural disorder at the solid–SmG transition is discussed and the changes are incorporated systematically.

1. Introduction

In recent years Raman spectroscopy has been a useful tool in the investigation of the vibrational dynamics of liquid crystalline compounds. The spectra–structure correlation, as well as the connection between structural phase changes and the corresponding changes in the Raman spectra, are of particular interest. These relationships have been used [1–8] to obtain information on different molecular configurations such as molecular orientation/rotation [9], intermolecular interaction and intramolecular charge transfer [10], etc.

The terepthalylidene-bis-*p*-*n*-alkylaniline (TBAA) homologous series is interesting because of its rich polymesomorphism and subtle properties [11, 12]. Of particular interest is the fact that the higher homologues, TB9A and TB10A, are the only non-ferroelectric thermotropic liquid crystals which exhibit a weakly first order smectic A–smectic C phase transition [13, 14]. Other interesting aspects of this homologous series are (i) the specific identification of SmG and SmH phases in a single compound [15, 16], (ii) the SmF and SmI phases [17, 18] and (iii) two or three second order phase transitions (SmA–SmC, SmI–SmF and SmF–SmG) in addition to the first order transitions in a single compound. Because the increasing chain length is the only distinguishing factor among the different compounds of this series, we report here a systematic and comparative room temperature Raman study of three liquid crystalline compounds TB4A, TB7A and TB10A. High temperature Raman spectra of certain spectral ranges are also reported in order to understand the complex phase behaviour of these compounds.

A detailed comparative spectroscopic analysis of the compounds of the TBAA series has not been reported so far, to the best of our knowledge. However, the laser Raman study of TB4A in various mesophases has been reported [1–4]. Most of these studies are at low temperatures, covering the low frequency (lattice mode) region. However, Schnur and Fontana reported [4] a few spectral anomalies of TB4A at higher temperatures viz. solid–smectic G and smectic G–smectic C transitions, but the associated changes in the spectral features have not been explained satisfactorily.

In view of the above, the present study emphasizes the following aspects: effect of chain length on molecular alignment, molecular stability whilst in solution, and inter/intra molecular orientation near phase transitions.

2. Experimental

The compounds TB4A, TB7A and TB10A were synthesized following the standard procedure [14–16] and recrystallized from an absolute ethanol–benzene mixture repeatedly until the observed transition temperatures were constant.

The transition temperatures were determined by using differential scanning calorimetry (DSC) and a polarizing microscope equipped with a hot stage. Special precautions were taken to prevent atmospheric hydrolysis, as the compounds of this homologous series are prone

*Author for correspondence.

to decomposition on prolonged heating in air at high temperatures.

The Raman spectra were obtained at room temperature for all three compounds in the range 400–1700 cm^{-1}, on a Spex Ramalog 1403 double monochromator equipped with RCA-31034 photomultiplier tube and CCD detector using the 488 nm line of an Ar^+ laser as excitation source. A slit combination of 200-400-400-200 μm, scanning increment of 0·1 cm^{-1} and integration time of 1·0 s were found suitable to record the spectra with a good signal-to-noise ratio. The samples were sealed into capillary tubes of 0·5–1 mm diameter, then placed in a specially made glass chamber which was subsequently evacuated. The temperature was continuously monitored and measured with an accuracy of ±0·1°C by placing a copper–constantan thermocouple in contact with the sample. Solution state spectra of TB4A, TB7A, TB10A were obtained by dissolving these compounds in carbon disulphide.

3. Results and discussion

The molecular structure and transition temperatures for the three compounds TB4A, TB7A, TB10A are shown below.

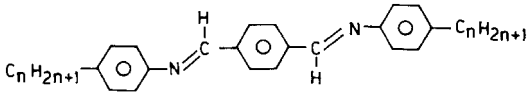

TB4A ($n=4$) Cr $\xrightarrow{112\cdot5}$ SmG $\xrightarrow{144\cdot0}$ SmC $\xrightarrow{172\cdot5}$ SmA $\xrightarrow{198\cdot5}$ N $\xrightarrow{235\cdot5}$ I (°C)

TB7A ($n=7$) Cr $\xrightarrow{61\cdot8}$ SmG $\xrightarrow{143\cdot0}$ SmF $\xrightarrow{156\cdot8}$ SmC $\xrightarrow{191\cdot4}$ SmA $\xrightarrow{210\cdot0}$ N $\xrightarrow{211\cdot6}$ I (°C)

TB10A ($n=10$) Cr $\xrightarrow{73\cdot0}$ SmG $\xrightarrow{120\cdot0}$ SmF $\xrightarrow{148\cdot4}$ SmI $\xrightarrow{153\cdot4}$ SmC $\xrightarrow{188\cdot3}$ SmA $\xrightarrow{190\cdot2}$ I (°C)

As shown above, the staggered core [11, 12] consists of three benzene rings connected by Schiff's base linkages, where the middle benzene ring is symmetrically substituted and the peripheral benzene rings are unsymmetrically substituted. The long unsaturated aliphatic chain attached to each side of the core has a zig-zag structure. However, the overall molecular structure is assumed to be *trans*-type.

As the present study aims to discuss the molecular dynamics (molecular orientation as well as rotation) and inter/intra-molecular interactions, we propose to categorize the discussion into two major parts: (1) comparison of the room temperature spectra of the three compounds in their solid and solution states, (2) comparison of the temperature dependent spectra of TB10A and TB4A in the range 1525–1650 cm^{-1} at the Cr–SmG transition.

3.1. *Room temperature spectra*

The room temperature spectra of TB4A, TB7A and TB10A in the range 400–1700 cm^{-1} are shown in figure 1, which reveals the spectral similarity between TB4A and TB7A and the dissimilarity in TB10A in comparison with the former two compounds. It is evident from figure 1 that the triplet structure of the TB10A spectra in the ranges 400–450, 600–700, 700–760 and 1500–1650 cm^{-1} coalesced to form a doublet or singlet in TB4A and TB7A, whereas the doublet nature of the ~950 and ~980 cm^{-1} bands, respectively, in TB4A and TB7A coalesced to form a singlet in TB10A. The 1563 cm^{-1} band is strong in TB10A whereas its 1417 cm^{-1} band is very weak; but in TB4A and TB7A, the 1563 cm^{-1} band appears just as a shoulder to the strong and sharp 1594 cm^{-1} band. However, a strong 1417 cm^{-1} band is already present in TB4A and TB7A. The alkyl chain length being the only difference between these three molecules, all the above observations point

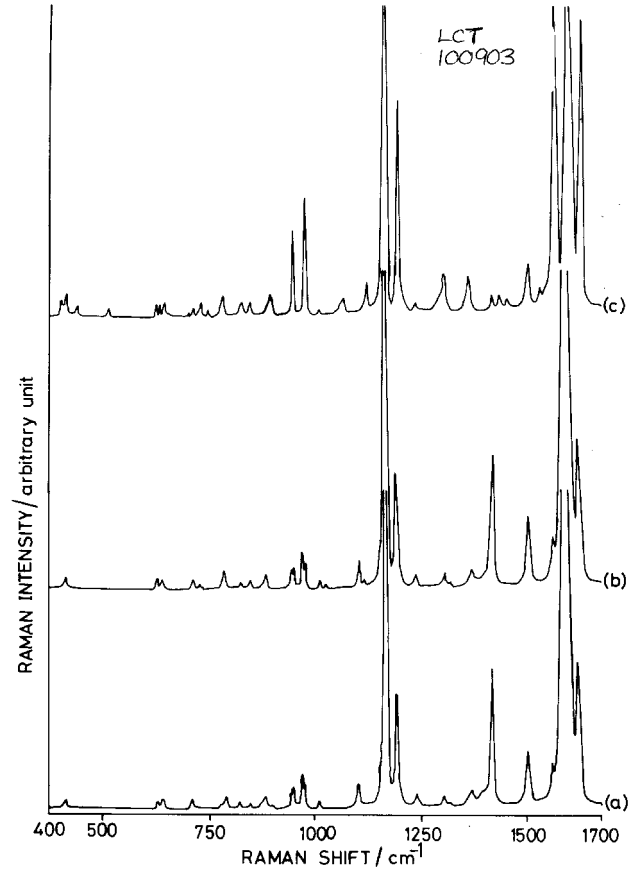

Figure 1. Relative intensity (I) of the 1240 cm^{-1} band with respect to the 980, 1167, 1193 and 1593 cm^{-1} bands.

towards the possibility of molecular disorder resulting from increased chain length. In order to understand the above spectral anomaly we propose a tentative assignment of different Raman modes by following the previous studies [19, 20] on similar compounds, depolarization ratios and expected group frequencies [21]. The assignments thus made are shown in table 1.

Figure 1 reveals that most of the spectral changes observed in the three compounds correspond to ring modes (also see table 1). However, a few of them are also alkyl chain modes (–CH_2– deformation, twisting, bending and rocking, etc.). Clearly, the changes observed in chain modes are due to the difference in chain length of the compounds. But changes in the ring modes associated with the backbone suggest a possibility that the backbone is affected by the increased chain length. This is supported by the weak appearance of the 1240 cm^{-1} band (C-aromatic–C-aliphatic stretching mode, $\nu_{\phi\text{-}C}$) in TB10A in comparison with TB4A and TB7A, showing the effect of alkyl chain stretching upon the peripheral benzene rings. In TB10A, the σ-electron cloud over the ϕ-C– bond (ϕ stands for benzene ring) distorted significantly and drifted towards the ring side as a result of stretching imposed by long alkyl chains

Table 1. A tentative assignment of Raman modes of TB4A, TB7A and TB10A in the spectral region 400–1700 cm^{-1}: abs = absent, ϕ = benzene ring, s = strong, sm = strong medium, m = medium, wm = weak medium, w = weak.

Peak position/cm^{-1}						
TB4A		TB7A		TB10A		
Solid	Solution	Solid	Solution	Solid	Solution	Assignment
413 (wm)		414 (wm)		404, 417, 455 (wm)		Out-of-plane aromatic C=C quadrant bending (16a)[a].
631, 645 (wm)		632, 645 (wm)		622, 638, 650 (wm)		In-plane aromatic C=C quadrant bending (16b).
714, 732 (w)		716, 733 (w)		716, 734, 751 (w)		Out-of-plane ring bending by sextant.
768, 784 (w)		788 (w)		785 (w)		
826 (w)		827 (w)		827 (w)		In-phase out-of-plane aromatic CH waging mode (17b).
852 (w)		851 (w)		858 (w)		
882, 900 (m)		886 (m)		889, 896 (m)		
944, 951 (sm)	948	946, 954 (sm)	942	948 (sm)	945	
973, 980 (sm)	969	974, 980 (sm)	969	978 (sm)	975 (wm)	Aromatic C=C stretching mode (breathing-mode) (18a).
1014 (w)	abs	1014 (w)	abs	abs (w)	abs	
1103 (m)	1100	1105 (m)	1100	1104 (m)	1098, 1161 (wm)	Aromatic in plane bending mode (9a, b).
1167 (s)	1161	1169 (s)	1162	1165 (s)		
1192 (sm)	1191	1193 (sm)	1191	1194 (sm)	1190	ϕ-N stretching mode.
1240 (w)	abs	1241 (w)	abs	1244 (w)	abs	ϕ-C stretching mode.
1305 (m)	1305	1305 (m)	1305	1305 (m)	1305	CH_2 twisting mode.
1366 (m)	1366	1369 (m)	1366	1366 (m)	1364	CH_2 deformation mode.
1418 (sm)	1416	1419 (sm)	1416	abs	1417, 1501 (wm)	Semicircle stretching mode (19a, b).
1504 (m)	1502	1505 (m)	1502	1503 (m)		
1563 (sm)	1561	1563 (sm)	1561	1564 (sm)	1560, 1593 (wm)	Aromatic quadrant stretching mode (8a, 8a′).
1588 (s)	1593	1588 (s)	1593	1595 (s)		
1621 (sm)	1625	1620 (sm)	1623	1624 (sm)	1625	C=N stretching mode.

[a] Wilson's notations of respective modes.

upon the backbone (especially on the peripheral benzene rings). This effect could easily be visualized by obtaining the relative intensity of the $\nu_{\phi\text{-}C}$ mode with respect to any prominent benzene ring mode.

Table 2 gives the intensity ratios of the 1240 cm^{-1} band with respect to the 980, 1167, 1193 and 1593 cm^{-1} bands (all benzene ring modes) in the three compounds. It is evident from the intensity ratios that there is a maximum charge distortion over the ϕ-C– bond in TB10A rather than in TB7A and TB4A, since the intensity of the associated stretching mode (1240 cm^{-1} band) is weak in TB10A.

In order to have a clear understanding of the structures of TB4A, TB7A and TB10A, the molecular packing of these molecules is taken into consideration, following X-ray studies on some compounds of the TBAA series [22–26]. According to these studies, compounds of the TBAA homologous series crystallize in a *c*-centred monoclinic lattice with a two-fold axis along the *b*-axis and molecular orientation along the *c*-axis (the *c*-axis being approximately half the molecular length). From this configuration it is clear that the molecular length stretches towards the *c*-axis and a layer forms along the *b*-axis. Again, the *b*-axis being two-fold and the backbone staggered, the most probable conformation is that the ring planes are oriented along the *ac*-plane. In such a situation chains of two neighbouring molecules will be closer along the *c*-axis and rings of two molecules will be closer along the *b*-axis.

As the chain length increases from TB4A to TB10A, the $-CH_2-$ groups will come closer along the *c*-axis and steric hindrance will stabilize them in such a way as to keep a minimum energy configuration. Simultaneously, the increased chain length will try to stretch the backbone making the staggered benzene rings relatively planar and thereby increasing the interplanar distance between the benzene rings of adjacent molecules. Hence the intermolecular interaction between the backbone decreases, resulting in splitting of the ring modes (see figure 1). However, this assumption is true for only out-of-plane aromatic C=C and C–H (both in- and out-of-phase) bending and stretching motions where an increase in interplanar distance facilitates these out of plane motions; the in-plane aromatic motions (C=C and C–H stretching) are not affected as such. The in-plane aromatic motions could only be affected by increasing intermolecular interaction or a reduction in the substituents along benzene rings. This is reflected by the doublet nature of the ~950 and ~980 cm^{-1} bands in TB4A and TB7A (molecules having shorter alkyl chains and lesser interplanar spacing), which coalesce to become singlets in TB10A (longer alkyl chain and wider interplanar spacing). However, the reasons for the weak appearance of the 1417 cm^{-1} band in TB10A and that of the 1563 cm^{-1} band in TB4A and TB7A, will be discussed in the next section.

Table 2. Relative intensity (I) of the 1240 cm^{-1} band with respect to the 980, 1167, 1193 and 1593 cm^{-1} bands.

Compound	$\frac{I_{1240}}{I_{980}}$	$\frac{I_{1240}}{I_{1167}}$	$\frac{I_{1240}}{I_{1193}}$	$\frac{I_{1240}}{I_{1593}}$
TB4A	0·340	0·038	0·12	0·032
TB7A	0·333	0·036	0·10	0·030
TB10A	0·050	0·018	0·03	0·015

If we consider that the above spectral anomalies are due to the difference in the compounds intermolecular interactions, then a system having negligible intermolecular interaction should give rise to similar spectra in the three compounds. This can be verified by obtaining the solution state spectra of the three compounds by dissolving them in carbon disulphide. Figure 2 shows the solution state Raman spectra of TB4A, TB7A and TB10A in the region 900–1700 cm^{-1}; there are equal numbers of Raman modes in all three compounds. Interestingly a 1417 cm^{-1} band (ν_{19b}) in TB10A and

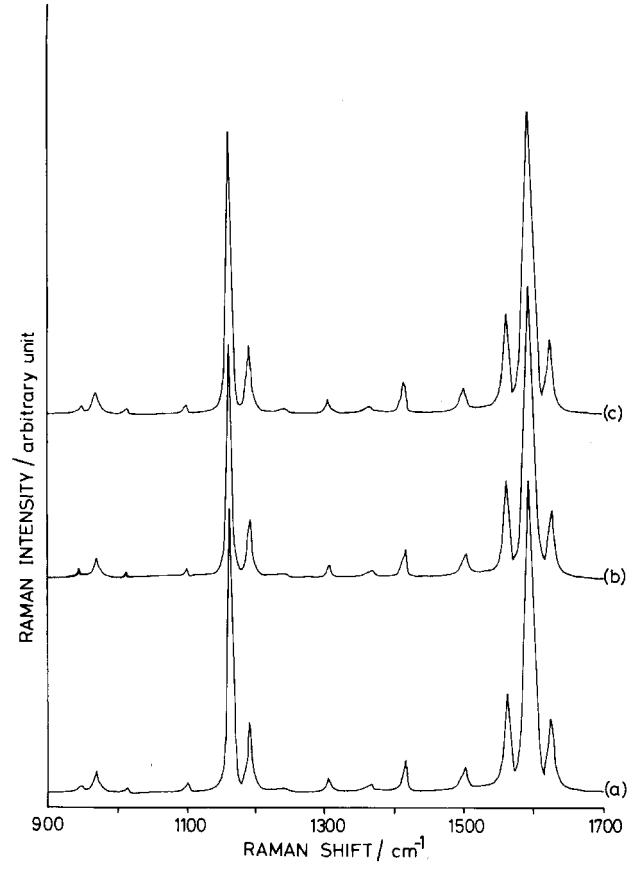

Figure 2. Solution state Raman spectra of (*a*) TB4A, (*b*) TB7A and (*c*) TB10A in the region 900–1700 cm^{-1}.

1563 cm^{-1} ($\nu_{8a'}$) band in TB4A and TB7A, which were absent in their solid states, appear in the solution state. This fact strongly supports the role of intermolecular interaction in the phenomenon of molecular vibrations. With restriction of movement being lifted in the solution state and intermolecular interaction being almost negligible, each segment of a molecule vibrates more freely. Therefore the number of Raman modes remains the same irrespective of any change in their molecular chain length. However, it should be noted here that the solution state spectra of these compounds in the region 400–900 cm^{-1} could not be recorded due to the presence of some very strong internal modes in this region.

Another important observation on the solution state is the shift of all the benzene ring modes, in all three compounds, towards lower frequencies (table 1). However the $\nu_{C=N}$ mode (1625 cm^{-1} band) shifts towards higher frequency and the position of modes associated with the alkyl chains remain unshifted. This indicates the loosening of ring bonds resulting in a decrease in bond energy [9], or the charge density on benzene rings might have drifted towards the C(H)=N– bond [10], thereby accounting for the shifting of the $\nu_{C=N}$ mode towards higher frequency (table 1). In the solution state, intermolecular interaction being negligible and without steric hindrance, the long alkyl chains will try to stabilize themselves in the lowest energy configuration by putting stress on the backbone. The backbone in this situation does not become planar, but rather is stabilized by the reorientation of peripheral benzene rings along the ϕ-N= bond [9]. In this changing environment, charge density over the peripheral benzene rings shifts towards the –C(H)=N– side along which no such motions are possible. However a contradiction is observed in TB4A and TB7A where the 1594 cm^{-1} band (ν_{8a}) shifted towards higher frequency in their solution state (see table 1). This discrepancy may be due to the weak appearance of the $\nu_{8a'}$ mode (a doublet partner of the ν_{8a} mode) in TB4A and TB7A in their solid state, for which the exact position of the ν_{8a} mode remains uncertain.

3.2. *Temperature dependent spectra of TB4A and TB10A*

In this study, Raman spectra of TB10A have been recorded in the wave number range 50–1700 cm^{-1} as a function of temperature, but only those regions which exhibit spectral changes during phase transitions are considered for the present discussion. The Raman spectra of TB10A at five different temperatures (near the Cr–SmG transition) and in the ranges 925–1025 and 1275–1475 cm^{-1} are shown in figure 3. The deconvoluted spectra of the region 925–1025 cm^{-1} at 90°C is shown as an inset. A comparison of temperature dependent

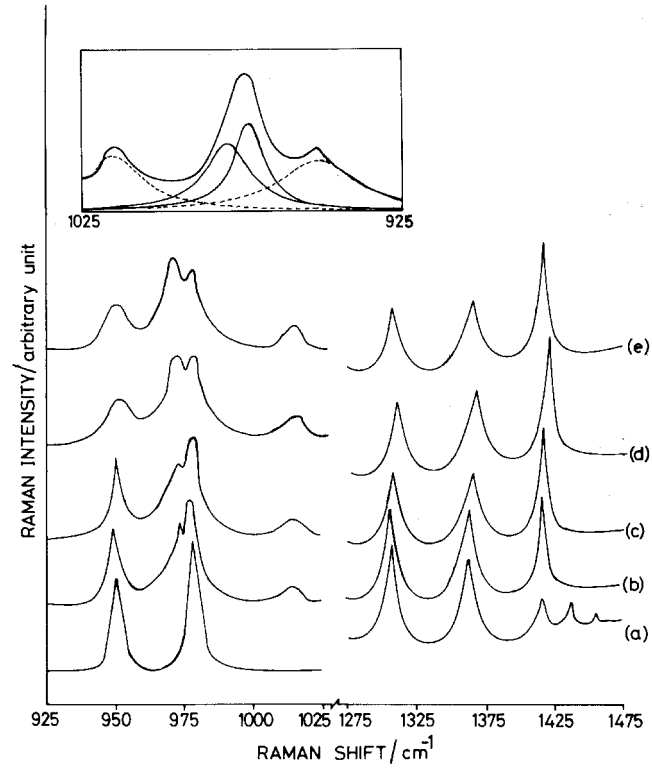

Figure 3. Temperature dependent Raman spectra of TB10A in the spectral regions 925–1025 and 1275–1475 cm^{-1} at (*a*) 30°C, (*b*) 70°C, (*c*) 72°C, (*d*) 73°C, (*e*) 78°C. The deconvoluted spectra of the region 925–1025 cm^{-1} at 90°C is shown as an inset.

spectra of TB4A and TB10A at two different temperatures (in solid and smectic G phases) is shown in figure 4. It is to be noted here that the temperature dependent spectra of TB4A at various ranges have already been reported [1–4]. However, here we have

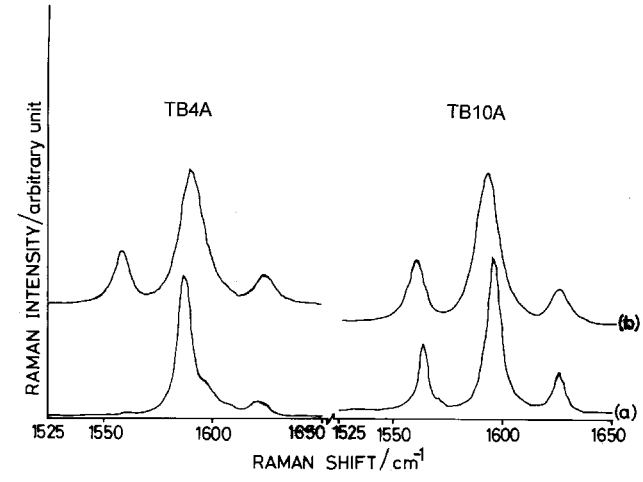

Figure 4. Temperature dependent Raman spectra of TB4A and TB10A in the spectral region 1525–1650 cm^{-1} at (*a*) 30°C, (*b*) 74°C.

chosen only the 1525–1650 cm^{-1} region in TB4A spectra, for the sake of comparison with TB10A. It can be seen from figure 3 that a peak appears at $\sim$1417 cm^{-1} during the Cr–SmG transition of TB10A which was very weak in its crystalline state. Also, the strong sharp band at $\sim$980 cm^{-1} (ν_{18a}) splits into a doublet (see figure 3) at the Cr–SmG transition and the intensity of the $\sim$950 cm^{-1} band (ν_{17b}) decreases rapidly as the Cr–SmG transition approaches. In order to understand these anomalies we would like to discuss the origin of these peaks in terms of their Raman activity, and the effect upon them of structural disorder during phase transition.

The ν_{19b} mode (1417 cm^{-1} band) has its origin in the semicircular stretching of benzene rings [21] where the *para*-substituted carbon atoms (C_1 and C_4) have an in-plane, unidirectional motion. This motion is shown in figure 5(*a*). In our systems, peripheral benzene rings play a major role in the appearance of this mode. The aforesaid motion becomes easier with a shorter alkyl chain attached to the peripheral benzene rings than with a longer chain. Hence the ν_{19b} mode is present in TB4A and TB7A, and absent in TB10A. Now during a Cr–SmG phase transition the molecules enter from a crystalline structure into pseudo-hexagonal packing with a local herringbone structure [16, 17]. Although the translational freedom between molecules is still very low in the SmG phase, the lateral gap existing between each pseudo-hexagonally packed cluster [12] creates a favourable environment for long alkyl chains to be more stretched along their molecular long axis, exerting stress on the backbone, especially on peripheral benzene rings. Such a situation facilitates the semicircular stretching motion of the benzene rings which in turn activates the ν_{19b} mode, and hence the 1417 cm^{-1} band becomes much stronger at the Cr–SmG transition for TB10A. This argument is supported by the appearance of the ν_{19b} mode in the solution state spectra of TB10A where the intermolecular interaction and steric hindrance are assumed to be much less. However the intensity of the 1417 cm^{-1} band continues to increase with temperature (see figure 3) due to increased fluidity.

The above argument also explains partially the splitting of the 980 cm^{-1} band at the Cr–SmG transition. This band has its origin in the ring-breathing mode (ν_{18a}) [21]. Due to the changing molecular environment during a Cr–SmG transition, as explained earlier, the breathing-frequency of peripheral benzene rings differs slightly from that of the middle ring. Therefore the 980 cm^{-1} band splits at the Cr–SmG transition of TB10A. A similar environment might have existed in TB4A and TB7A (having shorter alkyl chains) in their solid phase where the doublet nature of the $\sim$980 cm^{-1} band was observed. However, the splitting of this mode is observed for a very small temperature interval for TB10A. With increasing temperature the two peaks seem to coalesce to form a broad peak, in the same phase (S_G). This may be due to the induced planarity of the backbone resulting from increased fluidity, which creates an effectively similar environment for all the three benzene rings. But by deconvoluting the 980 cm^{-1} band in its coalesced form, the doublet nature is still observed (see figure 3). This doublet nature of the band remained in all the higher temperature phases of TB10A.

In figure 4, a peak has appeared at $\sim$1563 cm^{-1} ($\nu_{8a'}$) for TB4A at the Cr–SmG transition [3], whereas it was already present in the solid state spectrum of TB10A. Quadrant stretching of a benzene ring [21], where two *para*-substituted carbon atoms (C_1 and C_4) move radially opposite to each other, gives rise to this mode. Here also, the peripheral benzene rings are mostly involved in the appearance of this mode. This motion is shown in figure 5(*b*). In the solid phase, having a trivial close packed structure, there is hardly room for the aforesaid motion of the benzene ring [see figure 5(*b*)]. On reaching the SmG phase, whose structure has already been explained, the movement of *para*-substituted carbon atoms (C_1 and C_4) is facilitated, resulting in the appearance of the 1563 cm^{-1} band in TB4A. The above

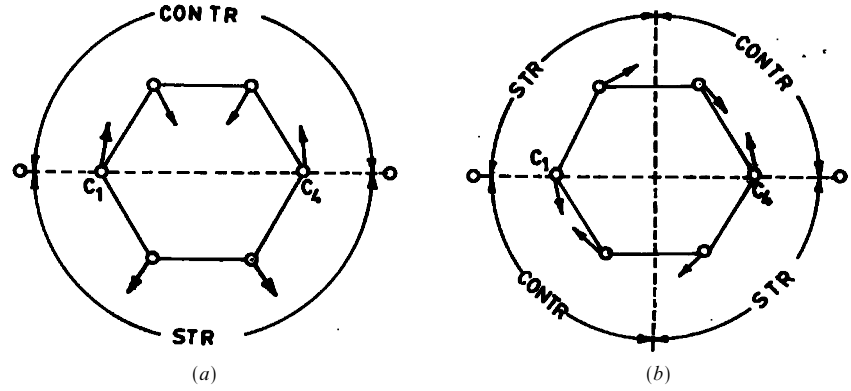

Figure 5. (*a*) Semicircular stretching mode of benzene ring; (*b*) quadrant stretching mode of benzene ring.

argument may seem confusing, as the 1563 cm^{-1} band is already present in the solid state spectra of TB10A, which has the longer alkyl chain. The explanation is that in TB10A the C_1 and C_4 carbon atoms are connected by long alkyl chains and Schiff's base linkages, because of which they remain immobile. However, the movement of other carbon atoms compensates this by fulfilling the condition of quadrant stretching as a whole. In TB4A, having the shorter alkyl chain, the C_1 atom has a little free movement, while the C_4 carbon atom remains stationary, thereby not fulfilling the quadrant stretching condition. This condition can only be fulfilled by a similar movement of C_4 carbon atoms, which is possible only when TB4A reaches its SmG phase. This argument is further supported by the appearance of this peak in spectra of TB4A in its solution state (see figure 2) where the intermolecular interactions are very small.

In conclusion, the effect of long alkyl chains plays a major role in molecular disordering in the different states (viz. solid, liquid, liquid crystalline) for the three compounds TB4A, TB7A and TB10A.

Financial support from the Department of Science and Technology, New Delhi, is acknowledged.

References

[1] Fontana, M., and Bini, S., 1976, *Phys. Rev. A*, **14,** 1555.
[2] Dvorjetski, D., Volterra, V., and Wiener-Avnear, E., 1975, *Phys. Rev. A*, **12,** 681.
[3] Schnur, J. M., Sheridan, J. P., and Fontana, M., 1975, in *Proceedings of International Liquid Crystal Conference* (*Pramana*, Supp. no. 1) edited by S. Chandrasekhar, p. 175.
[4] Schnur, J. M., and Fontana, M., 1974, *J. Phys. (Fr.)*, **35,** L-53.
[5] Bulkin, B. J., Grunbaum, D., Kennelly, T., and Loc, W. B., 1975, *Proceedings of International Liquid Crystal Conference* (*Pramana*, Supp. no. 1) edited by S. Chandrasekhar, p. 175.
[6] Schnur, J. M., 1973, *Mol. Cryst. liq. Cryst.*, **23,** 155.
[7] Amer, N. M., and Shen, Y. R., 1973, *Solid State Commun.*, **12,** 263.
[8] Sakamoto, A., Yosino, K., Kubo, U., and Inuishi, Y., 1974, *Jpn J. appl. Phys.*, **13,** 1691.
[9] Dash, S. K., Singh, R. K., Alapati, P. R., and Verma, A. L., *Mol. Cryst. liq. Cryst.* (in press).
[10] Dash, S. K., Singh, R. K., Bajpai, P. K., Alapati, P. R., and Verma, A. L., *Spectrochim. Acta* (submitted).
[11] Vertogen, G., and de Jeu, W. H., 1975, *Thermotropic Liquid Crystals: Fundamentals*, Springer series in Chemical Physics, Vol. 45.
[12] Gray, G. W., and Goodby, J. W., 1984, *Smectic Liquid Crystals: Textures and Structure* (London: Leonard Hill).
[13] Prasad, S. K., Raja, V. N., Shankar Rao, D. S., Nair, G. G., and Neubert, M. E., 1990, *Phys. Rev. A*, **42,** 2479.
[14] Alapati, P. R., Potukuchi, D. M., Rao, N. V. S., Pisipati, V. G. K. M., and Saran, D., 1987, *Mol. Cryst. liq. Cryst.*, **146,** 111.
[15] Sakagami, S., Takase, E. A., and Nakamizo, M., 1976, *Mol. Cryst. liq. Cryst.*, **36,** 261.
[16] Leibert, L., 1978, *Liq. Cryst. Solid State Phys. Suppl.*, **14** (New York: Academic Press).
[17] Goodby, J. W., Gray, G. W., and Mosley, A., 1978, *Mol. Cryst. liq. Cryst. Lett.*, **41,** 183.
[18] Diele, S., Demus, D., and Sackmann, H., 1980, *Mol. Cryst. liq. Cryst. Lett.*, **56,** 217.
[19] Vergoten, G., 1972, *Advances in Raman Spectroscopy*, edited by J. P. Mathieu (Hyden and Sons), Vol. 1, p. 219.
[20] Vergoten, G., and Fleury, G., 1976, *J. mol. Struct.*, **30,** 347.
[21] Clothup, N. B., Daly, L. H., and Wiberley, S. E., 1990, *Introduction to Raman and IR Spectroscopy* (Academic Press).
[22] Doucet, J., Levelut, A. M., and Lambert, M., 1972, *Phys. Rev. Lett.*, **32,** 301.
[23] Benattar, J. J., Doucet, J., Lambert, M., and Levelut, A. M., 1979, *Phy. Rev. A*, **20,** 2505.
[24] Benattar, J. J., Maussa, F., and Lambert, M., 1980, *J. Phys. (Fr.)* **41,** 1378.
[25] Leadbetter, A. J., Gauhan, J. P., Kelly, B., Gray, G. W., and Goodby, J. W., 1979, *J. Phys (Fr.)*, **40,** C3–178.
[26] Diele, S., Hartung, H., Ebeling, P., Vetters, D., Kruger, H., and Demus, D., 1980, *Advances in Liquid Crystals Research and Applications* (Oxford: Pergamon Press).